

Effect of fiber reinforcing on instantaneous deflection of self-compacting concrete one-way slabs under early-age loading

Behnam Vakhshouri* and Shami Nejadi

*Faculty of Engineering and Information Technology, School of Civil and Environmental Engineering,
University of Technology Sydney, Australia*

(Received January 7, 2017, Revised May 3, 2018, Accepted May 4, 2018)

Abstract. The Early-age construction loading and changing properties of concrete, especially in the multi-story structures can affect the slab deflection, significantly. Based on previously conducted experiment on eight simply-supported one-way slabs this paper investigates the effect of concrete type, fiber type and content, loading value, cracking moment, ultimate moment and applied moment on the instantaneous deflection of Self-Compacting Concrete (SCC) slabs. Two distinct loading levels equal to 30% and 40% of the ultimate capacity of the slab section were applied on the slabs at the age of 14 days. A wide range of the existing models of the effective moment of inertia which are mainly developed for conventional concrete elements, were investigated. Comparison of the experimental deflection values with predictions of the existing models shows considerable differences between the recorded and estimated instantaneous deflection of SCC slabs. Calculated elastic deflection of slabs at the ages of 14 and 28 days were also compared with the experimental deflection of slabs. Based on sensitivity analysis of the effective parameters, a new model is proposed and verified to predict the effective moment of inertia in SCC slabs with and without fiber reinforcing under two different loading levels at the age of 14 days.

Keywords: instantaneous deflection; early-age loading; one-way slab; reinforcement ratio; self-compacting concrete; effective moment of inertia; mixture design; fiber reinforcement; cracking moment; moment capacity; service moment

1. Introduction

Application of the Self-Compacting Concrete (SCC) is growing in many countries for different structural configuration and construction purposes. SCC is a type of high-performance concrete that can be produced with different mineral fillers and water reducing agents to facilitate the consolidation and proper filling of heavily reinforced and multipart formworks. Mechanical properties of the SCC is changing continuously from approximately liquid state to a visco-plastic material within a few hours, which is followed by further development into a hardened material with almost elastic properties.

There are limited investigations to compare the mechanical properties of SCC and conventional concrete (CC). However, deflection behaviour of the SCC and Fiber Reinforced SCC (FRSCC) members, especially at early-ages of concrete are not investigated in the literature, sufficiently. Aslani and Nejadi (2012) compared the CC and SCC material properties and reported a significant difference between the Modulus of Elasticity (MoE) and Tensile Strength (TS) in the range of Compressive Strength (CS) 45 to 80 MPa. However, for CS over 80 MPa, the difference was less.

Deflection control is a crucial parameter in serviceability design of the reinforced concrete slabs. The time-dependent and total deflections of slabs are generally

predicted on the basis of the instantaneous deflection at the time of loading. However, the early-age construction loading may have substantial changes from the required design loads.

In addition, majority of the existing models predict the instantaneous deflection for Conventional Concrete (CC) elements at the age of 28 days. While, deflection of flexural elements such as slabs with low reinforcement ratio is highly sensitive to the early-age loading during the construction and shrinkage-restraint stress (Scanlon and Bischoff 2008).

Combination of the early-age loading and application of the SCC as a new construction material complicates prediction of the instantaneous and time-dependent deflection in the lightly-reinforced concrete slabs. Different cracking behavior of the CC and SCC slabs also may affect the prediction of deflection in SCC and FRSCC slabs.

Cracking moment which has considerable effect on the time-dependent deflection can be reduced by shrinkage caused during the curing period before 28 days (Vakhshouri 2016). Moreover, insufficiency in the available data relating to the properties of SCC at early-age limits the deflection prediction of SCC structures.

Along with the errors associated with determination of the creep, shrinkage and material properties of concrete, a precise prediction of the instantaneous deflection is a major problem in calculation of the long-term and total deflection of one-way slabs (Vakhshouri and Nejadi 2014). A well-established method to predict the instantaneous deflection to include the early-age loading of the reinforced SCC elements and fiber reinforcing of the SCC mixtures is still

*Corresponding author, Researcher
E-mail: Behnam.vakhshouri@student.uts.edu.au

lacking in the literature.

The effective moment of inertia (I_e) is the most important parameter to estimate the instantaneous deflection of slabs. It includes the cracking effect of the slab section due to the applied loading and tension stiffening to accurate estimation of the flexural deflection in the slab. Some empirical models have been proposed in literature to estimate this parameter for particular type of structures and loading conditions. Faza and GangaRao (1992), Yost *et al.* (2003), Rafi *et al.* (2008), Alsayed *et al.* (2000) developed the I_e model for fiber reinforced CC beams, Hall and Ghali (2000) for CC beams. Fikry and Thomas (1998) also proposed the I_e models for both CC and fiber reinforced CC beams, and Benmokrane *et al.* (1996) for CC beams wrapped by fiber strips. However, more experimental researches are required to validate the proposed formulations and developing new models of the I_e for FRSCC members.

The American standards, ACI -209-08 and ACI-318-08 overestimate the MoE and underestimate the long-term deflection in CC slabs subjected to early-age loading (Park *et al.* 2010). Lee *et al.* (2007) conducted an experimental investigation on the slabs subjected to loading at the ages of 3, 7 and 28 days and concluded the significant effect of the early-age loading on the instantaneous and long-term deflection of slabs. They also showed the underestimated instantaneous and long-term deflections of the slabs at early-age loading due to the overestimation of the effective stiffness in ACI-318-08.

Mazzotti and Savoia (2009) observed a qualitative similar long-term deflection of the SCC and CC beams with substantial dependency of the time-dependent deflection both CC and SCC slabs on their instantaneous deflection. In addition, the existing codes of practice gave higher estimation of the total deflection in the CC and SCC beams. In SCC beams, the ratio of long-term to instantaneous deflection was 14 to 23% higher than the predictions of the investigated existing models.

This study investigates the instantaneous deflection of eight identical SCC slabs subjected to two distinct levels of the uniformly distributed gravity loading based on the previously conducted experimental data. The influence of loading level and the effective stiffness of the slab section on the instantaneous deflection at the age of 14 days ($\Delta_{inst-14}$) of the one-way SCC slab specimens are also evaluated. The test results and observations can be used to develop rational models for nonlinear analysis of the SCC slabs reinforced with different types of fibers.

The main objectives of this study are:

- Comparing the experimental values of $\Delta_{inst-14}$ in SCC and FRSCC slabs;
- Comparing the development of MoE and CS in SCC and FRSCC mixtures;
- Investigating the effect of time-dependent development of MoE on $\Delta_{inst-14}$;
- Comparing the experimental deflection with the calculated elastic deflection of slabs;
- Comparing the experimental deflections with predictions of the existing models of the effective moment of inertia (I_e) in codes of practice and empirical models;
- Investigating the effect of loading level, ratio of

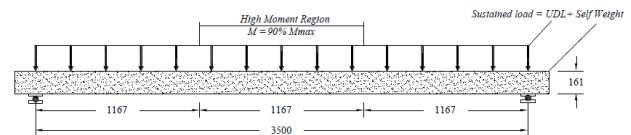


Fig. 1 Bar arrangement, cover details and dimension of slab specimens

the applied moment (M_a) to cracking moment (M_{cr}) and ultimate bending capacity of the slab section (M_u) on $\Delta_{inst-14}$;

(g) Investigating the effect of fiber type and content on the slabs deflection;

(h) Proposing and verification of the new I_e model to calculate the instantaneous deflection of SCC and FRSCC slabs at different loading levels at the age of 14 days.

2. Research significance

Determination and limitation of the time-dependent and consequently, the instantaneous deflection play critical roles in design of the lightly-reinforced concrete structures such as slabs. Therefore, accurate estimation of the instantaneous deflection strongly enriches the time dependent deflection prediction and consequently, makes an improved slab design.

Validity of the constitutive laws for the instantaneous and long-term behavior of SCC should be verified and the effect of early-age loading and fiber reinforcing of SCC slabs must be carefully checked.

The results of this investigation provide useful platform for engineers and researchers to develop new models and verification of the existing empirical equations for instantaneous deflection of the reinforced concrete slabs made with SCC and FRSCC mixtures.

3. Experimental investigation

3.1 Test program

Aslani *et al.* (2014) conducted series of tests on eight SCC slabs with four pairs of the mixture design at the concrete laboratory of the University of Technology Sydney (UTS). All slabs were internally reinforced with steel bars and different types of fiber. The slabs were constructed and tested to record the instantaneous deflection at mid-span. As shown in Fig. 1, all specimens were similarly simply-supported having length 3500 mm, depth 161 mm and width 400 mm. The side and bottom cover of concrete from the bar centroid were 40 and 25 mm, respectively.

Each slab was singly-reinforced with four symmetrically-positioned deformed N12 steel bars with 3800 mm length (including the anchorage length).

3.1.1 Curing and loading of slabs

Each slab was moist-cured for 14 days after casting and then subjected to loading. All slab specimens were subjected to different gravity loads, consisting of self-weight plus superimposed loads on top of the specimens. To



Fig. 2 Loading blocks arrangement and LVDT positioning for flexural test of SCC and FRSCC slabs

Table 1 Mixture design of slab specimens

Constituents	N-SCC	D-SCC	S-SCC	DS-SCC
Cement (kg/m ³)	160	160	160	160
Fly Ash (kg/m ³)	130	130	130	130
Ground-Granulated Blast-Furnace Slag (GGBFS) (kg/m ³)	110	110	110	110
Cementitious content (kg/m ³)	400	400	400	400
water	208	208	208	208
Water to cement ratio	0.52	0.52	0.52	0.52
Aggregate (kg/m ³)				
Coarse sand	660	660	660	660
fine sand	221	221	221	221
Coarse aggregate	820	820	820	820
Admixtures(lit/m ³)				
Super plasticizer	4	4.86	4.73	4.5
Viscosity modifying agent	1.3	1.3	1.3	1.3
High range water reducing agent	1.6	1.6	1.6	1.6
Fiber content (kg/m ³)				
Steel	-	30	-	15
Polypropylene	-	-	5	3

Table 2 Physical and mechanical properties of fibers used in the SCC mixtures

Type	Steel	Polypropylene
Trade name	Drami x RC-80/60-BN	Synmi x 65
Density (kg/m ³)	7850	905
Length (l)	60	65
Diameter (d)	0.75	0.85
Aspect Ratio (l/d)	80	76.5
Tensile strength (MPa)	1050	250
Elasticity modulus (GPa)	200	3

provide the required loading, rectangular concrete blocks of predetermined size and weights were cast and weighed prior to the commencement of the test. Slab specimens were uniformly loaded by the concrete blocks using wooden timbers as loading pads. The deflection at mid-span of the slab specimen was recorded by a Linear Variable Differential Transformer (LVDT). Each LVDT was placed

Table 3 Mechanical properties of the SCC and FRSCC mixtures at 14 and 28 days

	Age (day)	N-SCC	D-SCC	S-SCC	DS-SCC
Compressive strength (MPa)	14	29.05	34.3	32.45	38.1
	28	33.3	38	38.1	45
Modulus of Elasticity (GPa)	14	32.24	29.14	29.68	31.26
	28	35.39	35.76	35.76	36.1
Density (kg/m ³)		2340	2274	2330	2385

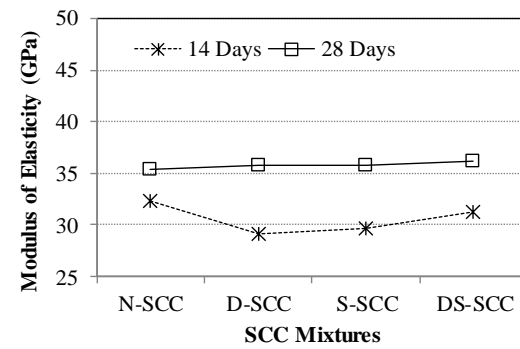
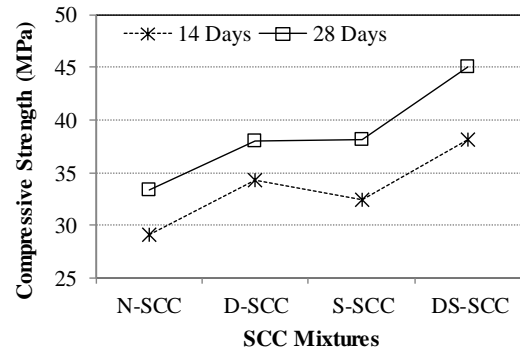


Fig. 3 Compressive strength and modulus of elasticity of SCC mixtures at two ages of 14 and 28 days

at mid-span under the slab in equal distances from the supports. Fig. 2 shows the arrangement of the concrete blocks on top surface of the slabs and the position of LVDTs under the slabs.

3.2.2 Mixture design and components

Eight simply supported one-way SCC slabs have been subjected to service loads to investigate the instantaneous deflection at mid-span of the slab at the age of 14 days. For this purpose, two plain SCC slabs (N-SCC), two steel fiber reinforced SCC slabs (D-SCC), two polypropylene fiber reinforced SCC slabs (S-SCC) and two hybrid fiber reinforced SCC slabs (DS-SCC) have been considered in the test program. Table 1 explains the mixture design in SCC and FRSCC slabs. Type and volume of the fibers that strongly influence the mechanical properties of the SCC mixtures are illustrated in Table 2.

4. Early-age properties of SCC and FRSCC mixtures

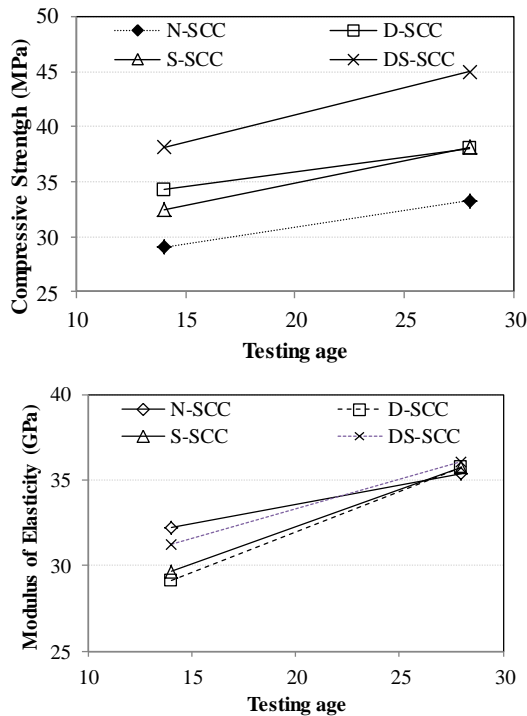


Fig. 4 Development of CS and MoE of SCC mixtures with time

Table 4 Section properties, load levels, predicted elastic deflection and experimental instantaneous deflection

Slab	w_a (KN/m)	M_u (KN.m)		M_a (KN.m)	M_a / M_u (%)		Δ_e (mm)		Δ_{ins} (mm)
		14 days	28 days		14 day	28 day	14 day	28 day	
N-SCC-a	7.31	27.47	27.78	11.189	40.73	40.27	3.18	2.9	12.1
N-SCC-b	5.41	27.47	27.78	8.28	30.14	29.8	2.36	2.15	5.89
D-SCC-a	7.26	27.84	28.05	11.12	39.94	39.65	3.5	2.85	7.65
D-SCC-b	5.36	27.84	28.05	8.21	29.48	29.27	2.58	2.11	7.59
S-SCC-a	7.3	27.73	28.05	11.18	40.32	39.85	3.45	2.87	6.41
S-SCC-b	5.4	27.73	28.05	8.27	29.83	29.48	2.55	2.12	2.91
DS-SCC-a	7.33	28.05	28.34	11.23	40.03	39.63	3.29	2.85	8.98
DS-SCC-b	5.43	28.05	28.34	8.32	29.66	29.36	2.44	2.11	5.14

Existing models in the literature give under or overestimated values of the mechanical properties of concrete. In addition, the models to predict the early-age properties of SCC are very rare in the literature. Therefore, exact values of CS, MoE and density of the mixtures have been measured by test specimens in the laboratory conditions at two ages of 14 and 28 days, as presented in Table 3. According to the test results, all mixtures are classified as normal-weight and normal-strength SCC.

Sukumar *et al.* (2008) compared the early-age compressive strength of high-volume fly ash SCC with those of CC and found that increasing rate of the CS in SCC is slightly higher. The ratio of CS in SCC at the age of 28 days to that of 14 days was 1.15 in their experiment.

Figs. 3 and 4 compare the experimental values of the CS and MoE and their development with time in the SCC and FRSCC mixture at the ages of 14 and 28 days.

According to Figs. 3 and 4, the N-SCC mixture poses the lowest values of the CS at both ages. The initial value and development rate of the CS in the DS-SCC mixture are the highest quantities, compared to those of the other mixtures. Development of CS in N-SCC and S-SCC mixtures is similar, while D-SCC mixture has the lowest rate of CS increment with time. The average ratio of CS at 28 days to 14 days in SCC mixtures (with and without fiber) is 1.15. This ratio confirms the results of experiment by Sukumar *et al.* (2008).

The experimental values of the MoE at the age of 28 days in all mixtures are very similar; however, the MoE values at the age of 14 days are different. The N-SCC and D-SCC mixtures have the highest and lowest values of the MoE at the age of 14 days, respectively. While, the lowest and highest development rate of the MoE are seen in the N-SCC and D-SCC mixtures, respectively. The average development rate of MoE in the SCC mixtures (with and without fiber) is 1.17. As a general conclusion, the mixtures with fiber reinforcing show higher development rate of the CS and MoE with time.

The growing rate in this study is defined as the difference between the MoE values at the ages of 14 and 28 days in 14 days. According to Table 3 and Fig. 4, MoE in N-SCC is changing from 32.24 to 35.39 GPa within 14 days and the growing rate is $(35.39-32.24)/(28-14)=0.225$ GPa/day. While, this rate for D-SCC is $(35.76-29.14)/(28-14)=0.473$ GPa/day.

5. Difference between elastic and instantaneous deflection of SCC slabs

The instantaneous deflection of slabs was recorded by a LVDT installed at mid-span of the slab, immediately after loading (placing all loading blocks on the slab) at the age of 14 days. Table 4 shows the estimated elastic deflection (Δ_e) and experimental instantaneous deflection of the slabs subjected to two different levels of the uniformly distributed load (w_a). The experimental MoE values at the ages of 14 and 28 days are utilized to estimate the Δ_e at those ages. The ultimate flexural capacity of the slab section (M_u), applied moment (M_a) due to the self-weight and external loading and the ratio of M_a/M_u are also given in Table 4. The ultimate moment capacity of reinforced concrete section in each pair of slabs is calculated theoretically considering equivalent stress block of singly-reinforced section.

Some simplified methods in the design codes may use the elastic deflection as the basis of the total and time-dependent deflection calculations. However, considering the instantaneous deflection as elastic deflection is a common source of the errors in design of the concrete structures. Fig. 5 shows the ratio of the experimental instantaneous deflection to the estimated elastic deflection at the ages of 14 days (Δ_{ins}/Δ_e)₁₄ and 28 days ($\Delta_{ins-14}/\Delta_{e-28}$) in the SCC and FRSCC slabs. The ratio of (Δ_{ins}/Δ_e)₁₄ in the slabs varies between 1.14 in slab S-SCC-b to 3.8 in slab N-SCC-a. Comparing the recorded deflection at 14 days (Δ_{ins-14}) with the estimated elastic deflection at 28 days (Δ_{e-28}), the ratio of $\Delta_{ins-14}/\Delta_{e-28}$ ranges from 1.37 in slab S-SCC-b to 4.178 in

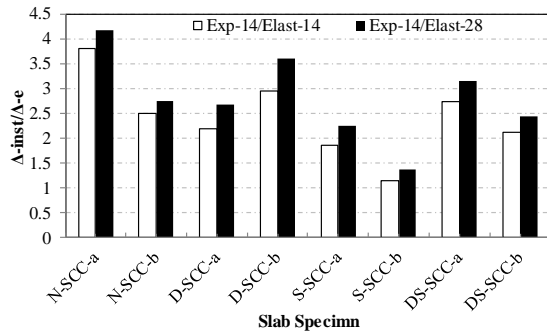


Fig. 5 Ratio of experimental instantaneous deflection at 14 days to estimated elastic deflection at 14 and 28 days

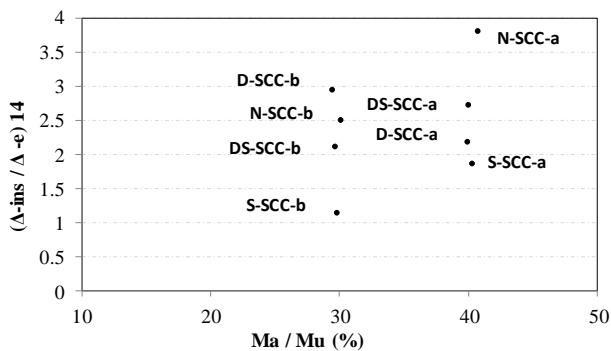


Fig. 6 Instantaneous/elastic deflection ratio of slabs at 14 days under two different ratios of M_a/M_u

slab N-SCC-a. As a matter of fact, the increased flexural stiffness of the slab at the age of 28 days decreases the elastic deflection and consequently, increases the ratio of $\Delta_{ins-14}/\Delta_{e-28}$. Majority of the Δ_{ins}/Δ_e ratios at both ages are in the range of 2 to 3. The average ratios of $(\Delta_{ins}/\Delta_e)_{14}$ and $\Delta_{ins-14}/\Delta_{e-28}$ are 2.4 and 2.79, respectively. In this range the FRSCC slabs are mostly below the average and the SCC slabs are above the average. Improving effect of the fiber reinforcing in the FRSCC mixture to enhance the flexural stiffness of the slabs is the main reason to explain this behavior.

6. Effect of loading level on the instantaneous deflection

Since the slabs are identical, the ratio of applied moment to the flexural capacity of the slab section (M_a/M_u) plays a major role in comparison of the instantaneous deflection of the lightly-reinforced SCC and FRSCC slabs. This effect becomes more critical for early-age loading of the slabs. Fig. (6) compares the effect of M_a/M_u on the ratio of $(\Delta_{ins}/\Delta_e)_{14}$ in the slabs. Two loading levels are about 30% and 40% of the ultimate bending capacity ($0.3M_u$ and $0.4M_u$) in each pair of the slabs with the same mixture design. Unexpectedly, the effect of 10% higher M_a/M_u ratio on the Δ_{ins-14} is considerable in these identical slabs.

Except for the slabs D-SCC (a, b), 10% load increment causes 30% to 63% higher $(\Delta_{ins}/\Delta_e)_{14}$ ratio in the DS-SCC and S-SCC slabs, respectively. In the N-SCC slabs, the ratio of $(\Delta_{ins}/\Delta_e)_{14}$ is increasing about 53% due to 10% load increment.

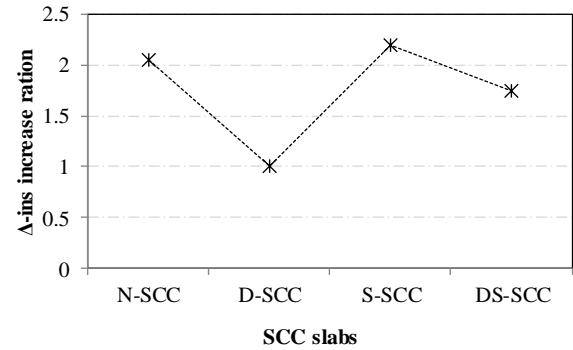


Fig. 7 Increasing ratio of Δ_{ins-14} due to 10% increase in M_a/M_u ratio

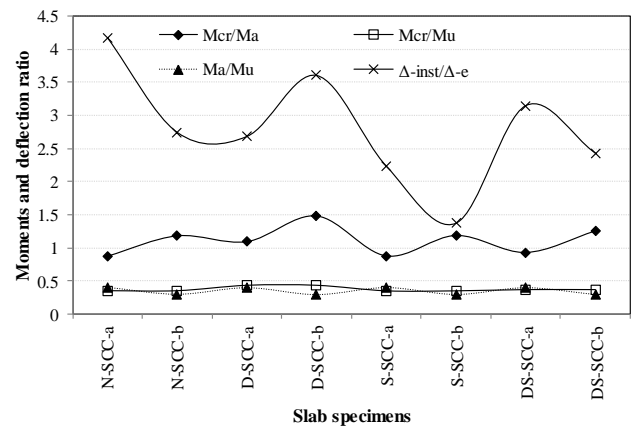


Fig. 8 Effect of moment ratios on Δ_{ins}/Δ_e at 14 days

Despite similar values of the Δ_{ins-14} in the D-SCC slabs, the estimated elastic deflection under two different loading levels varies about 36%. Accordingly, the ratio of $(\Delta_{ins}/\Delta_e)_{14}$ decreases about 25% in the D-SCC slabs by 10% higher M_a/M_u ratio. The average increment of the $(\Delta_{ins}/\Delta_e)_{14}$ ratio by 10% higher M_a/M_u ratio in all slabs is about 30%.

Increasing the Δ_{ins-14} due to variation of the M_a/M_u ratio is different from the variation of $(\Delta_{ins}/\Delta_e)_{14}$ in the slabs. In average, 10% higher M_a/M_u ratio, causes about 75% growth in Δ_{ins-14} of all eight slabs; while, this load increment causes about 25% higher Δ_{ins-14} in the FRSCC slabs.

The individual increasing ratio of Δ_{ins-14} under two different loading levels in the N-SCC, D-SCC, S-SCC and DS-SCC slabs are 2.05, 1.008, 2.2 and 1.74, respectively. In other words, the early-age instantaneous deflection of the N-SCC, S-SCC and DS-SCC slabs is significantly sensitive to the load magnitude. Fig. 7 shows the increasing ratio of the early-age instantaneous deflection of slabs due to increased ratio of the M_a/M_u .

Along with the magnitude of the applied moment, effect of the cracking moment (M_{cr}) that causes the first cracking is considerable in deflection calculations of the slabs. M_{cr} and M_u are dependent characteristics of the section and consequently, they may change the Δ_{ins}/Δ_e ratio in a similar manner. In addition, the ratio of M_a/M_u in the presented experiment is limited to 30% and 40% in the slabs. In other words, M_a is dependent to a fraction of M_u in this study.

Variation of the Δ_{ins}/Δ_e ratio at the age of 14 days with different ratios of the applied moment, moment capacity

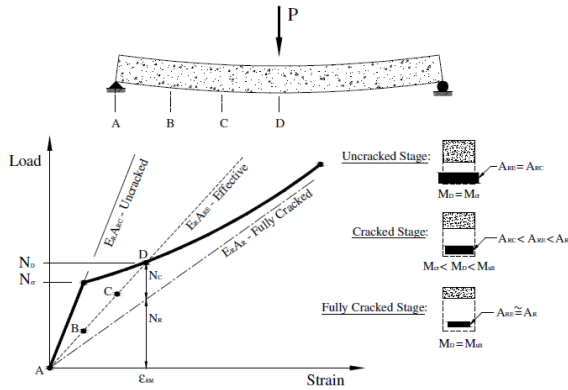


Fig. 9 Deformation response of idealized reinforcement at critical section (Gilbert 2007)

and cracking moment of the slab section is presented in Fig. 8. Despite very small changes in the ratios of M_{cr}/M_u and M_a/M_u in the slabs, the Δ_{ins}/Δ_e ratio shows considerable changes in the slabs.

The applied M_a is less than the M_{cr} in most of the slabs (5 out of 8 slabs), in which, the section is expected to behave in the elastic range. However, due to the creep and shrinkage effects and initiation of the cracking in tension zone, the experimental instantaneous deflection is higher than the estimated elastic deflection. As presented in Fig. 8, the instantaneous deflection in the slabs increases slightly by decreasing the ratio of M_{cr}/M_a ; while, the growing ratios of the M_{cr}/M_u and M_a/M_u amplify the instantaneous deflection of the slabs.

7. Effective moment of inertia

The principle factors that affect the instantaneous deflection of the reinforced concrete members under flexural loads are MoE, load magnitude, load distribution and support conditions. In addition, continuity of the sections along the span; i.e., variable cross-sections and hence, variable moment of inertia depending on the degree of cracking along the slab strongly influence the instantaneous deflection of slab.

When an RC element cracks, its stiffness does not suddenly change to that of a section where the tension-concrete can be fully disregarded (Gilbert 2007). In fact, the sections where the cracks are localized are separated by regions where the concrete in tension is uncracked with an increment of the stiffness. Behavior at the cracked section used to compute the cracked transformed moment of inertia (I_{cr}) is assumed to be linear elastic, and nonlinearity of the member stiffness is taken into account with I_e that models the transition from a gross (uncracked) moment of inertia (I_g) to I_{cr} . Fig. 9 explains the deformation response of a simply-supported slab in three stages of uncracked, cracked and fully-cracked section under sustained service loading. M_a and M_u are the applied moment and the ultimate moment capacity of the reinforced concrete section, respectively. The effective stiffness (EA) for uncracked, cracked and fully-cracked sections is presented in the figure.

Reference	Equation	Application	Expression
(Faza and GangaRao 1992)	$I_m = \frac{23I_{cr}I_g}{8I_{cr}+15I_g}$ (1)	FRP beam	I_e from ACI-318
(Rafi et al. 2008)	$I_e = \left(\frac{M_{cr}}{M_a}\right)^3 \beta_d I_g + \left[1 - \left(\frac{M_{cr}}{M_a}\right)^3\right] \frac{I_{cr}}{\gamma}$ (2) $\gamma = \left(\frac{0.0017\rho}{\rho_h} + 0.8541\right) \left(\frac{E_f}{2E_s} + 1\right)$	FRP members	
(Alsayed et al. 2000)	$I_e = I_{cr}$ for $\frac{M_{cr}}{M_a} > 3$ (3) $I_e = \left[1.4 - \frac{2}{15} \left(\frac{M_{cr}}{M_a}\right)\right] I_{cr}$ (4) $\leq I_g$ for $1 < \frac{M_{cr}}{M_a} < 3$	FRP members	
(Hall and Ghali 2000)	$I_e = \frac{I_g I_{cr}}{I_{cr} + [1 - \beta_1 \beta_2 \left(\frac{M_{cr}}{M_a}\right)^2] (I_g - I_{cr})}$ (4)	Normal concrete	$\beta_1=1$: ribbed and 0: smooth bars $\beta_2=1$: first and 0: sustained loading
(Fikry and Thomas 1998)	$I_{cr}^{-M_a/M_{cr}} (L_{cr}/L)^{\rho} \leq I_g$ for $\rho > 1\%$ (5) $I_e = I_{cr} + (I_g - I_{cr})^{-M_a/M_{cr}} (L_{cr}/L)^{\rho}$ (6)	FRP and Normal concrete	L_{cr} : Cracked length L : Length of member ρ : Reinforcement ratio
(Benmokrane et al. 1996)	$I_e = \left(\frac{M_{cr}}{M_a}\right)^3 \frac{I_g}{7} + 0.84 \left[1 - \left(\frac{M_{cr}}{M_a}\right)^3\right] I_{cr} \leq I_g$ (7)	FRP beam	
Bronson (1963) Bronson (1965) (Vakhshouri and Nejadi 2014)	$I_e = \left(\frac{M_{cr}}{M_a}\right)^2 I_g + (1 - \left(\frac{M_{cr}}{M_a}\right)^2) I_{cr} \leq I_g$ (8) $I_e = \left(\frac{M_{cr}}{M_a}\right)^3 I_g + (1 - \left(\frac{M_{cr}}{M_a}\right)^3) I_{cr} \leq I_g$ (9) $I_e = \left(\frac{M_{cr}}{M_a}\right)^4 I_g + (1 - \left(\frac{M_{cr}}{M_a}\right)^4) I_{cr} \leq I_g$ (10)	Normal concrete	Power in expressions: 2: Initially expected 3: Average member behavior 4: Section behavior
Bischoff (2005, 2007) Bischoff and Scanlon (2007) (Vakhshouri and Nejadi 2014)	$I_e = \frac{I_{cr}}{1 - \eta \beta \left(\frac{M_{cr}}{M_a}\right)^2} \leq I_g$ (11) no tension stiffening $0 \leq \beta \leq 1$ full tension stiffening	Flexural members	
(Alshaiikh and Al-Zaid 1993)	$I_e = I_{cr} + (I_g - I_{cr}) \left(\frac{M_{cr}}{M_a}\right)^{3-0.8\rho} \leq I_g$ (12)	Point load on beams	ρ : tensile reinforcement ratio
ACI318-08 435-66 ((ACI) 2008) AS-3600-09 (Standards 2009)	$I_e = \left(\frac{M_{cr}}{M_a}\right)^3 I_g + (1 - \left(\frac{M_{cr}}{M_a}\right)^3) I_{cr} \leq I_g$ (13)	Normal concrete	$I_e \leq 0.6I_g$ in AS3600-09 proposed by Gilbert (2001) for lightly reinforced members
(Bischoff and Gross 2010)	$I_{ef} = \frac{I_{cr}}{1 - \eta \beta \left(\frac{M_{cr}}{M_a}\right)^2} \leq I_g$ (14) $\gamma = 1.72 - 0.72 M_{cr}/M_a$, $\beta = M_{cr}/M_a$	Simply supported uniform load	Equivalent moment of inertia
(Bischoff and Gross 2010) (EUROCODE 1994)	$I_e = \frac{I_{cr}}{1 - \eta \left(\frac{M_{cr}}{M_a}\right)^2} \leq I_g$ (15) $\eta = 1 - I_{cr}/I_g$	Originally for axial tension members	Applicable for flexural members
ACI 440 (2006)	$I_e = \left(\frac{M_{cr}}{M_a}\right)^3 \beta_d I_g + \left[1 - \left(\frac{M_{cr}}{M_a}\right)^3\right] I_{cr} \leq I_g$ (16) $\beta_d = \alpha_{\beta} \left(\frac{E_f}{E_s} + 1\right)$, $\beta_d = 0.2 \frac{\rho}{\rho_h} < 1$	FRP members	E_f : Elasticity of FRP bars E_s : Elasticity of steel bars
ACI 440 (2006) and (Yost et al. 2003)	$I_e = \left(\frac{M_{cr}}{M_a}\right)^3 \beta_d I_g + \left[1 - \left(\frac{M_{cr}}{M_a}\right)^3\right] I_{cr} \leq I_g$ (17) $\beta_d = 0.2 \frac{\rho}{\rho_h} < 1$	FRP members	
(Newhook 2001)	$I_e = \frac{I_g I_{cr}}{I_{cr} + [1 - 0.5 \left(\frac{M_{cr}}{M_a}\right)^2] (I_g - I_{cr})} \leq I_g$ (18)	FRP members	
(Darwin et al. 1986)	$A_e = \left(\frac{p_{cr}}{p}\right)^3 A_g + (1 - \left(\frac{p_{cr}}{p}\right)^3) A_{cr} \leq I_g$ (19) A_g : Gross cross section area, cr : nA_s	Members under direct tension	Analogous approach for I_e in ACI-318

Branson (1963) introduced and developed (1965) the concept of using the effective moment of inertia to predict the curvature and deflections directly from the elasticity theory. The concept then was verified by different researchers and organization mainly by implementing the idea of tension stiffening to apply for different types of structures, loading rates, section reinforced with fiber and Fiber Reinforced Polymer (FRP) sheets and FRP bars (Achintha and Burgoyne 2009, Vakhshouri and Nejadi 2014). Eqs. (1) to (19) present some verified models of the

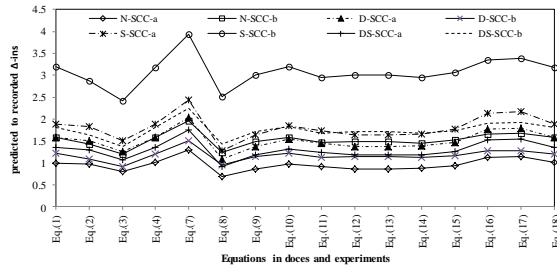


Fig. 10 Comparison of the recorded and predicted instantaneous deflection of SCC and FRSCC slabs at 14 days

I_e to enhance the prediction of the instantaneous deflection in the reinforced concrete members. Some of these equations have been proposed for special conditions such as point loading, concrete members with FRP bars and near surface mounted FRP strips. However, their predictions have been compared with the experimental Δ_{ins-14} values in this study to monitor any compatibility in between.

The estimated values of the I_e by using the Eqs. (1) to (18) have been utilized to predict the instantaneous deflection of SCC and FRSCC slabs at the age of 14 days. The experimental Δ_{ins-14} in the slabs has been compared and evaluated with these predicted deflection values in Fig. 10.

There are considerable differences between the predicted and experimental instantaneous deflection of slabs in majority of the models. Eq. (8) (Branson’s model) is the initial version of almost all other investigated models; however, according to Fig. 10 it gives better estimation of the instantaneous deflection of the slabs, in general. While, the Eq. (7) shows considerable overestimation of the instantaneous deflection in all the slabs. The average ratio of the predicted to experimental Δ_{ins-14} in the Eqs. (8), (3), (17) and (7) is 1.26, 1.32, 1.87 and 2.14, respectively. The ratio for all other equations is in the range of 1.53 and 1.84.

Considering the utilized concrete type and loading levels, the Δ_{ins-14} in the slab N-SCC-a is overestimated by 6% to 32% in nine studied models; while, the Δ_{ins-14} in D-SCC-b and DS-SCC-a slabs is overestimated about 5% by Eq. (8). The instantaneous deflection values in other slabs are generally overestimated by 5% to 218% by the existing models.

The Δ_{ins-14} in slab N-SCC-a is well-predicted by the Eqs. (1), (2), (7), (14) and (17); however, it is considerably underestimated by the Eqs. (8) and (9). The average value of the predicted Δ_{ins-14} for the slabs N-SCC-b and D-SCC-a is close to the experimental data. Instantaneous deflection of the S-SCC slabs is considerably overestimated in all equations, and the average ratio of predicted to recorded Δ_{ins-14} in S-SCC (a), (b) slabs is 1.81 and 3.1, respectively. According to Fig. 4, the modulus of elasticity of the S-SCC mixture at the age of 14 days is considerably lower than that of 28 days. In other words, the lower stiffness of the S-SCC slabs in the early-age causes bigger difference between the predicted and experimental deflection values.

Predictions of the investigated existing models for the DS-SCC slabs are higher than the experimental instantaneous deflection values. However, they are better than the predicted values for D-SCC and S-SCC slabs. The

Table 5 Coefficients and limitations of proposed for I_e model

I_e, ρ, M_a	Coefficient of fiber type (α)	Ratio of elasticity β	Fiber content V_f
$I_e \leq 0.6I_g$ $\rho \geq 0.005$ $M_{cr}/M_a < 3$	$\alpha=0.9$	$\beta = E_{c-14}/E_{c-28}$ E _{c-14} and E _{c-28} Modulus of elasticity of concrete at 14 and 28 days	Fiber volume fraction in the mixture (Kg/m ³) presented in Table 1
	for DS-SCC		
	$\alpha=1.0$		
	for SCC		
	$\alpha=1.15$		
	for D-SCC		
$\alpha=1.95$	for S-SCC		

average ratio of the predicted to experimental Δ_{ins-14} in DS-SCC-a, b slabs is 1.29 and 1.75, respectively. Eqs. (3) and (8) give better prediction of the Δ_{ins-14} in the slab DS-SCC-a; while, the predictions by Eqs. (7) and (17) are far from the experimental Δ_{ins-14} . In the slab DS-SCC-b, the estimated Δ_{ins-14} by the Eqs. (3) and (17) are 38% and 125% higher than the experimental Δ_{ins-14} . The overestimated Δ_{ins-14} in the slab S-SCC-b by other I_e models is between the above-mentioned extreme points.

8. Proposed analytical model

There are several analytical and numerical models in the literature to predict the I_e in CC and fiber reinforced CC members. These models vary in precision in the estimation and complexity. However, in regard to SCC and FRSCC members, no evidence of such models is found.

Comparative investigation of the presented models and experimental data show that the models in the Eqs. (7) and (17) give conservative Δ_{ins-14} predictions of the SCC and FRSCC slabs. In this study, the required certain intrinsic and/or extrinsic variables (i.e., properties of concrete, support conditions, loading type and age) in I_e prediction is well covered by the presented equations. In addition, the Eq. (8) (as basis of the other latter studies) and Eq. (3) give the closest predictions to the recorded experimental data. Considering the Eqs. (3) and (8) as base of the proposed model in this study, of the time-dependent elasticity of concrete, fiber volume fraction in the mixture, ultimate and cracking moment capacity of the slab section and the applied moment on the slab are included in the new model. These parameters are implemented to get a precise estimations of the instantaneous deflection of the SCC and FRSCC slabs with different values of the gravity loading at early-ages of the concrete. The fiber type, fiber volume fraction and the aspect ratio of fiber are the main effective parameters to evaluate the fiber reinforced sections, especially in tensile and flexural behavior. Considering the negligible difference in the aspect ratio of the applied fibers in the FRSCC slabs, effect of the type and volume fraction of the fiber on the instantaneous deflection of the slab is investigated. In addition, according to considerable effect of the time-dependent M_u on the moment ratios and the instantaneous deflection in Figs. 6 and 7, the M_{cr}/M_u ratio is also included in the developed model in this study. To include the effect of early-age loading, the ratio of MoE of concrete at loading age to the MoE at the age of 28 days is implemented in the model.

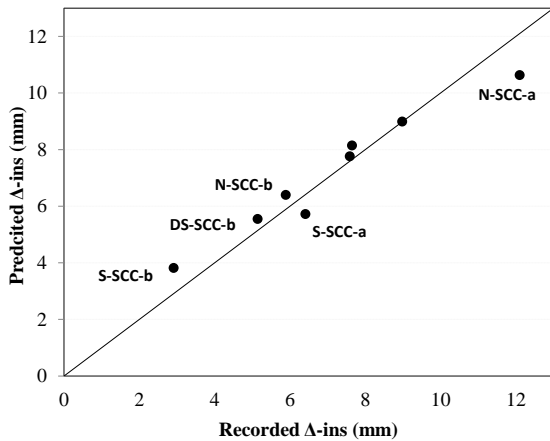


Fig. 11 Comparison of the experimental and predicted instantaneous deflection of slabs at the age of 14 days

Eqs. (3), (8) are basically developed for deflection prediction of the reinforced concrete beams. Eq. (3) predicts the I_e in two distinct ranges of $1 < M_{cr}/M_a < 3$ and $M_{cr}/M_a > 3$. In addition, there is no limit for the M_{cr}/M_a ratio in the Eq. (8). The ratios of M_{cr}/M_a and M_{cr}/M_u for the slabs in this study are ranging between 0.87-1.48 and 0.35-0.43, respectively. Accordingly, the proposed equation is recommended to apply for $M_{cr}/M_a < 3$.

Eq. (20) is proposed to predict the I_e in SCC and FRSCC slabs. The implemented coefficients and limitations of the Eq. (20) are illustrated in Table 5.

$$I_e = \alpha \times I_{cr} \left(\frac{M_{cr}}{M_a} \right)^{(1-0.1V_f)} + \left[(1 - \beta) + \frac{M_{cr}^2}{(M_a \times M_u)^{(2+\beta)}} \right] I_g \quad (20)$$

Where; M_{cr} is the cracking moment (KN.m), M_a is the applied moment (KN.m), I_{cr} is the moment of inertia in a cracked section (m^4), I_g is the gross moment of inertia (m^4), V_f is fiber volume in the mixture (kg/m^3), β is the ratio of MoE at loading age to the MoE at 28 days, and α is an experimental coefficient. The experimental coefficients are taken from the multi-linear regression analysis to adopt the proposed model with the experimental data.

Excluding the steel bars from the reinforced concrete section causes about 17% underestimation of the I_g of the slabs in this study. Therefore, the transformed section method is utilized to include the reinforcement to calculate a precise value of the I_g of the uncracked section in the SCC and FRSCC slabs.

Fig. 11 compares the experimental Δ_{ins-14} of the slabs with prediction of the proposed model by applying the corresponding coefficients. Obviously, the predicted values in all slabs are in a good agreement with the experimental data.

Fig. 10 compares the experimental deflection values with predictions of the existing models in the literature. Since the proposed model is developed on the basis of the best-matching models in Fig. 10, it can be concluded that combination of the Figs. 10 and 11 can give a comparison of the proposed model with the models in Eqs. (1) to (18).

Table 6 Comparison of experimental deflection with predictions of the proposed model and Eqs. (3) and (18)

	N-SCC-a	N-SCC-b	D-SCC-a	D-SCC-b	S-SCC-a	S-SCC-b	DS-SCC-a	DS-SCC-b
Eq. (3)	0.98	1.59	1.54	1.22	1.85	3.20	1.32	1.82
Eq. (8)	0.92	1.46	1.45	1.12	1.73	2.95	1.24	1.68
Eq. (20)	0.88	1.09	1.06	1.02	0.89	1.31	1.00	1.08

Table 6 compares the ratio of the predicted deflection of the slab by Eqs. (3), (8) and (20) to the experimental deflection values in the slabs.

9. Conclusions

The early-age loading of slabs is inevitable in most construction projects. In addition, the structural behavior of the SCC and FRSCC slabs is not completely understood in the literature. These parameters complicate the prediction of deflection of early-age loaded slabs. This study investigated the effect of M_{cr} , M_a and M_u on the instantaneous deflection of SCC and FRSCC slabs. Correspondingly, the effect of time-dependent changes of the MoE of SCC mixtures with and without fiber, and the load levels on the instantaneous deflection of slabs were studied.

The existing I_e models in the CC members with and without fiber reinforcing were utilized to predict the Δ_{ins-14} of the SCC and FRSCC slabs in this study. The best-matching equations were selected as the basis of the new proposed model to predict the I_e in the SCC and FRSCC slabs at the early-age loading. Including the effect of time-dependent MoE of concrete, fiber volume fraction in the mixture, fiber type and M_{cr}/M_u ratio were the main modifications on the selected basic models to adopt with the experimental data. The proposed model predicted the I_e values and consequently, the Δ_{ins-14} of the SCC and FRSCC slabs, accurately.

The following conclusions can be drawn from the study:

- Early-age instantaneous deflection of the SCC and FRSCC slabs can be predicted by the proposed model in this study with high accuracy;
- Fiber reinforcing improves the MoE and CS of the SCC slabs and consequently, reduces the instantaneous deflection at early-age loading. Development of the mechanical properties of the FRSCC mixtures with time is higher than that of the SCC mixtures. The DS-SCC and S-SCC mixtures have the highest development of the CS and MoE, respectively;
- Considering the elastic deflection equal to instantaneous deflection even in the range of $M_{cr} > M_a$ is a common source of error in the concrete structures design. The Δ_{ins-14} in majority of the slabs in this study is about 2 to 3 times the Δ_{e-14} . This ratio for the FRSCC slabs is lower than that for the SCC slabs;
- The effect of load increment on the Δ_{ins-14} is different in different slabs. Increasing the M_a/M_u ratio by 10% changes the $(\Delta_{ins}/\Delta_e)_{14}$ ratio by 30%, in average. However, variation of the Δ_{ins-14} under two loading levels of the $M_a/M_u=0.3$ and 0.4 is surprisingly higher than the variation

of the ratio of $(\Delta_{ins}/\Delta_e)_{14}$;

- The increased load in the N-SCC, D-SCC, S-SCC and DS-SCC slabs caused 105%, 7%, 120% and 74% greater Δ_{ins-14} , respectively. In average, the 10% higher M_a/M_u ratio caused about 76% higher Δ_{ins-14} in the SCC slabs;

- The M_{cr}/M_u ratio showed a great effect on Δ_{ins-14} of the slabs, especially, in the slabs made with a mixture without fiber.

References

- Achintha, P.M. and Burgoyne, C.J. (2009), "Moment-curvature and strain energy of beams with external fiber-reinforced polymer reinforcement", *ACI Struct. J.*, **106**(1), 20-29.
- ACI-318-08 (2008), *Building Code Requirements for Structural Concrete ACI-318-08*, American Concrete Institute, Farmington Hills, Michigan, U.S.A.
- Alsayed, S., Al-Salloum, Y. and Almusallam, T. (2000), "Performance of glass fiber reinforced plastic bars as a reinforcing material for concrete structures", *Compos. Part B: Eng.*, **31**(6), 555-567.
- Alshaikh, A.H. and Al-Zaid, R. (1993), "Effect of reinforcement ratio on the effective moment of inertia of reinforced concrete beams", *Struct. J.*, **90**(2), 144-149.
- Aslani, F. and Nejadi, S. (2012), "Mechanical properties of conventional and self-compacting concrete: An analytical study", *Constr. Build. Mater.*, **36**, 330-347.
- Aslani, F., Nejadi, S. and Samali, B. (2014), "Long-term flexural cracking control of reinforced self-compacting concrete one way slabs with and without fibres", *Comput. Concrete*, **14**(4), 419-443.
- Benmokrane, B., Chaallal, O. and Masmoudi, R. (1996), "Flexural response of concrete beams reinforced with FRP reinforcing bars", *ACI Struct. J.*, **93**(1), 46-55.
- Bischoff, P.H. and Gross, S.P. (2010), "Equivalent moment of inertia based on integration of curvature", *J. Compos. Constr.*, **15**(3), 263-273.
- Darwin, D., Scanlon, A., Gergely, P., Bishara, A.G., Boggs, H.L., Brander, M.E., Carlson, R.W., Clark Jr, W.L., Fouad, F.H. and Polvika, M. (1986), "Cracking of concrete members in direct tension", *ACI J. Proc.*
- EUROCODE, N. (1994), *8: Design Provisions for Earthquake Resistance of Structures*, Part 2: 1998-1992.
- Faza, S. and GangaRao, H. (1992), "Pre- and post-cracking deflection behaviour of concrete beams reinforced with fibre-reinforced plastic rebars", *Proceedings of the 1st International Conference on Advance Composite Materials in Bridges and Structures (ACMBS-I)*, Canadian Society of Civil Engineers, Sherbrooke, Canada.
- Fikry, A.M. and Thomas, C. (1998), "Development of a model for the effective moment of inertia of one-way reinforced concrete elements", *Struct. J.*, **95**(4), 445-455.
- Gilbert, I.R. (2007), "Tension stiffening in lightly reinforced concrete slabs", *J. Struct. Eng.*, **133**(6), 899-903.
- Hall, T. and Ghali, A. (2000), "Long-term deflection prediction of concrete members reinforced with glass fibre reinforced polymer bars", *Can. J. Civil Eng.*, **27**(5), 890-898.
- Lee, J., Scanlon, A. and Scanlon, M. (2007), "Effect of early age loading on time-dependent deflection and shrinkage restraint cracking of slabs with low reinforcement ratios", *Spec. Publ.*, **246**, 149-166.
- Mazzotti, C. and Savoia, M. (2009), "Long-term deflection of reinforced self-consolidating concrete beams", *ACI Struct. J.*, **106**(6), 772.
- Newhook, J. (2001), *Reinforcing Concrete Structures with Fibre*

- Reinforced Polymers*, T. C. N. o. C. o. e. o. i. s. f. i. Structures, Manitoba, Canada, ISIS Canada: Design Manual No.3, **3**.
- Park, H., Hwang, H., Kim, J., Hong, G., Im, J. and Kim, Y. (2010), "Creep and effective stiffness of early age concrete slabs", *Proceeding of the Fracture Mechanics of Concrete and Concrete Structures-Assessment, Durability, Monitoring and Retrofitting of Concrete Structures*, Jeju, South Korea.
- Rafi, M.M., Nadjai, A., Ali, F. and Talamona, D. (2008), "Aspects of behaviour of CFRP reinforced concrete beams in bending", *Constr. Build. Mater.*, **22**(3), 277-285.
- Scanlon, A. and Bischoff, P.H. (2008), "Shrinkage restraint and loading history effects on deflections of flexural members", *ACI Struct. J.*, **105**(4), 498.
- Standards, A. (2009), *Concrete Structures*, AS-3600-09, Standards Australia, Australia.
- Sukumar, B., Nagamani, K. and Raghavan, R.S. (2008), "Evaluation of strength at early ages of self-compacting concrete with high volume fly ash", *Constr. Build. Mater.*, **22**(7), 1394-1401.
- Vakhshouri, B. (2016), "Time-dependent bond transfer length under pure tension in one way slabs", *Struct. Eng. Mech.*, **60**(2), 301-312.
- Vakhshouri, B. and Nejadi, S. (2014), *Limitations and Uncertainties in the Long-Term Deflection Calculation of Concrete Structures. Vulnerability, Uncertainty, and Risk: Quantification, Mitigation, and Management*, ASCE.
- Yost, J.R., Gross, S.P. and Dinehart, D.W. (2003), "Effective moment of inertia for glass fiber-reinforced polymer-reinforced concrete beams", *Struct. J.*, **100**(6), 732-739.

CC

Note

Eqs. (21), (22) are utilized to determine the elastic deflection of slabs under two levels of loading values and M_{cr} , respectively.

$$\Delta_e = \frac{5}{384} \times \frac{W_a \cdot l^4}{E_c \cdot I_g} \quad (21)$$

$$M_{cr} = I_{cr} \times f_r \quad (22)$$

Where; W_a , l , E_c , I_g , I_{cr} and f_r are uniformly distributed load (KN/m), span length (m), MoE of concrete (KN/m²), gross moment of inertia (m⁴), cracking moment of inertia (m⁴) and modulus of rupture (KN/m²), respectively.